Algal Research 49 (2020) 101945

Contents lists available at ScienceDirect

Algal Research

journal homepage: www.elsevier.com/locate/algal

Engineering bacteria-seaweed symbioses for modulating the photosynthate content of *Ulva* (Chlorophyta): Significant for the feedstock of bioethanol production

Mark Polikovsky[a,*], Gianmaria Califano[b], Nico Dunger[b], Thomas Wichard[b], Alexander Golberg[a,*]

[a] Porter School of the Environment and Earth Sciences, Tel Aviv University, Israel
[b] Institute for Inorganic and Analytical Chemistry, Friedrich Schiller University Jena, Germany

ARTICLE INFO

Keywords:
Axenic culture
Bioethanol
Monosaccharides
Symbioses
Seaweed-associated bacteria
Ulva mutabilis
Flux balance analysis

ABSTRACT

Seaweed biomass cultivation predicates the quantity and quality of this biorefinery feedstock. Unfortunately, the seaweed growth rate and chemical content are hardly predictable and are affected by environmental factors, including epiphytic bacteria. We hypothesize that microbiome engineering can control the chemical composition of *Ulva* biomass. We show that the engineered *Maribacter* sp. and *Roseovarius* sp. consortium modulate *Ulva mutabilis* growth rate and photosynthate content of constituents relevant for bioethanol production. Although minimal growth was observed in the axenic cultures (0.04 mm day^{-1}), *Ulva mutabilis* in a tripartite community showed a growth rate of 3.79 mm day^{-1} in the growth phase. Furthermore, the content of glucose and glycerol in *Ulva* of the engineered community increased by 77 ± 19% and 460 ± 207% whereas xylose and glucuronic acid decreased by 37 ± 14% and 46 ± 15% in comparison to axenic culture.

Interestingly, bacterial addition affected the rhamnose/xylose/glucuronic acid ratio (1.96:1:1: vs 1.34:0.85:1 in xenic vs axenic culture), indicating the impact of bacteria on ulvan synthesis. In addition, tyrosine and histidine increased by 191 ± 61% and 40 ± 26%; however, valine, isoleucine, aspartate, threonine, serine, and phenylalanine decreased by 22 ± 19% - 42 ± 23%. Flux-balance analysis of *Saccharomyces cerevisiae*, *Escherichia coli*, and *Clostridium acetobutylicum* was used to estimate the bioethanol yield from hydrolyzed *Ulva* biomass, in a one-step or two-step fermentation process. Simulation using *S. cerevisiae* (RN1016) with xylose isomerase resulted in a bioethanol yield of 85.62 for xenic vs. 71.31 mg/g dry weight (DW) axenic cultures of *Ulva*.

The increased growth rate and the relative amounts of photosynthates of *U. mutabilis* are modulated by the engineered microbiome. Moreover, it results in biomass with a higher potential for bioethanol fermentation in comparison to axenic cultures.

1. Introduction

Conventional fossil sources for energy supply have adverse side effects of climate change [1,2]. Terrestrial plants, which are current alternative feedstocks for biofuels, conflict with food production [3]. Moreover, the agriculture for cultivating those plants is contributing to water consumption, greenhouse gas emissions, and the degradation of natural environments [4,5].

Seagriculture emerges as an alternative to agriculture practice to produce seaweed biomass for the sustainable biofuel feedstock supply chain [6–8]. In seagriculture, green, red, and brown seaweed biomass could massively be cultivated in seawater. Thus, seagriculture does not compete for arable land or potable water [9,10].

From all green macroalgae species, *Ulva* spp. are particularly attractive as a potential biomass feedstock for biorefinery [7,11] due to its rapid growth rate [6] and adaptation to varied habitats with different abiotic conditions [12,13]. *Ulva*'s carbohydrates are composed mainly of C5 and C6 monosaccharides, iduronic acid, and glucuronic acid [14–16]. The monosaccharides derived from *Ulva* biomass could be fermented into bioethanol, a versatile chemical, and biofuel [11,15].

However, the chemical content and the composition in *Ulva* sp. varies between the species and is influenced by seasonality and other environmental abiotic and biotic conditions [17–20]. This fluctuation in the chemical composition of the biomass, challenge the optimization of efficient fermentation processes [21]. Therefore, control of the macroalgae biomass chemical composition is required. This control

* Corresponding authors.
E-mail addresses: markpolikovsky@gmail.com (M. Polikovsky), agolberg@tauex.tau.ac.il (A. Golberg).

https://doi.org/10.1016/j.algal.2020.101945
Received 19 November 2019; Received in revised form 7 May 2020; Accepted 11 May 2020
Available online 23 May 2020

could improve the yield of the downstream biomass conversion to biofuels. Even though the power of abiotic environmental parameters is commonly investigated for seaweed aquaculture [22–24], the understanding of the biological microenvironment [25] is still understudied.

Indeed, the natural microbiome of seaweeds plays an intricate role in the algal physiology [26], nutrition, metabolism [27], and immune function [28]. The seaweeds have a proper surface and chemosphere, which may serve as an attractive environment for the bacterial existence [26,27,29]. This environment includes beneficial compounds for bacterial growth such as oxygen [30], carbon source, nutrients [29,31], and metabolites [28]. Recent studies explicitly investigated the cross-kingdom interactions between *Ulva* spp. and its associated bacteria [26]. Metabolomics research compared the chemosphere of axenic *U. mutabilis* culture with a tripartite community of *U. mutabilis* and its two naturally associated bacteria, *Roseovarius* sp. strain MS2 and *Maribacter* sp. strain MS6. Bacteria can recognize *Ulva* as a reliable food source through chemoattractants [32]. In turn, bacteria induce algal growth and morphogenesis settling around the algal holdfast [32]. Bacteria of the *Rosoebacter* clade often promote algal growth to develop their own (bacterial) benefits [33].

The photosynthate secreted by *Ulva* spp. includes carbon sources such as glycerol [31]. Notably, the glycerol is the backbone of triacylglycerols (TAG) and the primary form of energy storage in plants [34]. These storage lipids are essential to plant development, being used, for example, in seedling growth during germination [35]. As glycerol is essential for both algal and bacterial growth, we hypothesize that algal growth- and morphogenesis promoting bacteria trigger the sugar and glycerol production of *Ulva mutabilis* in standardized algal aquacultures.

Moreover, we also tested, whether bacteria modulate the amino acids (AAs) pattern of *Ulva*, due to their potential role in the *Ulva*'s morphogenesis. Such modulation of photosynthate is essential not only for *Ulva* growth and development but also for the utilization of *Ulva* and its downstream processing, such as bioethanol fermentation. For testing these hypotheses, we applied a targeted analysis of organic compounds critical for bioethanol production in *Ulva* tissue such as monosaccharides, glucuronic acid, glycerol, and AAs. The engineered tripartite community composed of *U. mutabilis* with *Roseovarius* sp. and *Maribacter* sp. was compared with the *U. mutabilis* axenic culture. The chemical content of *U. mutabilis* from these two cultures types served as feedstocks for a flux balance analysis of bioethanol fermentation in BioLego. This specially designed software that uses flux balance analysis (FBA) to predict bioethanol yield from biomass with various fermenting microorganisms [36]. Our study demonstrates that engineering of *Ulva*'s microbiome leads to a better understanding of the bacterial role in the macroalgal biomass production, critical for developing an efficient seaweed-based biorefinery.

2. Materials and methods

2.1. Induction of U. mutabilis gametes

The cultivation was carried out as previously described by Alsufyani et al. (2017) for 63 days [31]. The fast-growing natural developmental mutant of *U. mutabilis* Føyn (mating type mt+; morphotype "slender" (sl)) was cultivated [37,38]. The *Ulva* cultivation was started from haploid gametes to achieve reproducibility and synchronization of the algae. For preparing the *Ulva* seed stock, gametogenesis was induced in mature thalli (a four weeks old culture started from gametes). Gametogenesis was induced by fragmentation with a herb chopper (Zyliss, Zurich, Switzerland) into smaller fragments (1–3 mm size) (Fig. S1A). Sporulation inhibitors were removed from the *Ulva* tissues with the immersion of the fragments three times in 50% artificial seawater [39]. After three days of cultivation, the *Ulva* culture medium (UCM) was changed for removing the swarming inhibitor that led to the gametes discharge.

2.2. Preparation axenic gametes

The feedstock of *U. mutabilis* axenic germlings was prepared by separating gametes from the associated bacteria in Pasteur pipettes under strictly sterile conditions using the phototactic properties of the gametes. This method is a standard operational procedure (Fig. S1B) [40]. The axenicity of the gametes was tested by plating 10 μL of the gametes seed stock on marine broth (Roth, Germany) agar plates (1.5%; *w/v*) (Sigma-Aldrich, Germany) and by performing polymerase chain reactions (PCR) of the 16S rRNA gene [41]. Gametes were counted by flow cytometry. About 6×10^3 axenic gametes were inoculated as seed stock in 250 mL sterile UCM in polycarbonate tissue culture flasks (V = 650 mL, BD Falcon, Franklin Lake, NJ, USA). The feedstock was incubated for 24 h in the dark for settlement of the gametes [31,40].

2.3. Engineering U. mutabilis and bacteria symbioses

Algae were cultured under light: dark (17:7 h) regime and the illumination of a photon flux of 60–120 (μmol $m^{-2}{\cdot}s^{-2}$) (50% GroLux, 50% daylight fluorescent tubes; OSRAM, München, Germany) at 18 °C. Sock cultures of the two bacterial strains, *Roseovarius* sp. (MS2) (Genbank EU359909) and *Maribacter* sp. strain (MS6) (Genbank EU359911) [41], were grown on the orbital shaker at 20 °C in liquid marine broth medium (Roth, Germany). For preparing the tripartite community of *U. mutabilis* and two associated bacteria (i.e., the xenic cultivation), the exponentially growing bacterial cultures were harvested by centrifugation (3000 × *g*) for 5 min. The cell pellet was resuspended and washed three times with sterile UCM. Finally, the two bacterial strains were added to the axenic gametes of *Ulva* [31] (Fig. S1C). The bacterial suspension was diluted to a final optical density (OD) of 0.001 in the cell tissue flask.

After 14 days of cultivation of *Ulva* in tissue flasks, propagules of the xenic and axenic cultures were transferred to the 25-l polycarbonate bottles (i.e., bioreactors) filled with 15 L UCM. The experiment was started with 5×10^3 germlings for both treatments, while for the tripartite community preparation, each bacterial inoculum was added (OD_{620nm} = 0.0001, OD in the bioreactor after inoculation). Half of the culture medium was renewed after 4 weeks. *Ulva* was collected from the tripartite community and axenic cultures equivalent to 100–350 mg dry weight (DW) after 8 weeks of cultivation . Each culture, tripartite community or axenic culture, was cultivated in three independent replicates.

The growth rate (mm day^{-1}) was calculated by a length with the following equation:

$$Growth\ Rate\ (mm\ day^{-1}) = \frac{L_t - L_0}{T_t - T_0}$$

L = length (in mm), T = time (in days). t = time of the cultivation. The parameters of the growth rate during the growth phase (T_t = 35 and T_0 = 7 days after inoculation in the bioreactor) of *Ulva* in tripartite community and axenic culture were; L_t = 117.11 mm, L_0 = 10.9 mm, and L_t = 1.06 mm, L_0 = 0.01 mm.

2.4. Biomass hydrolysis for the quantification of monosaccharides, glucuronic acid, and glycerol

Biomass was dried (16 h) at 50 °C in an oven (Fig. S1D) and subsequently grounded into powder using mortar and pestle. The powder was then stored at −28 °C. For every biological replicate, a duplicate of hydrolysis treatment was performed. Thermochemical hydrolysis [42] was conducted with 2% sulfuric acid (*v*/v) for 30 min at 121 °C in a ratio of 1:250 (solid: solvent) using 10 mL autoclavable centrifuge tubes (Nalgene™ Oak Ridge High-Speed PPCO Centrifuge Tubes, ThermoFisher Scientific, CA) in the autoclave (Tuttnauer 2540MLV, Netherlands). Each batch, 4 ± 0.5 mg of dried biomass was weighed (Mettler Toledo, Switzerland). Sulfuric acid (Sigma-Aldrich, Israel) was diluted

to 2% (v/v) and was added to the tube. Hydrolysates were stored at 4 °C. Triplicate of algae samples were hydrolyzed in duplicate before being analyzed (Fig. S1E).

2.5. Monosaccharides quantification

The monosaccharides were determined (Figs. S1F, 2) by high-pressure ion chromatography (HPIC) according to a protocol of Robin et al. (2017) with small adaptations [43]. In brief, aliquots of the hydrolysates were taken and diluted in ultrapure water before being filtered through a 0.22 μm syringe-filter (Millipore, USA) in HPIC vials (Thermo Fischer Scientific, MA, USA). Monosaccharide content in the hydrolysates were measured by high-performance anion exchanged chromatography with pulsed amperometric detection (HPAEC-PAD) using a Dionex ICS-5000 platform (Dionex, Thermo Fischer Scientific, MA, USA) equipped with an analytical column (Dionex™ AminoPac™ PA10 IC) and a guard column (Thermo Fischer Scientific, UK). An electrochemical detector with an AgCl reference electrode was used for measuring the compounds. The analysis was performed using an isocratic flow gradient of 100–4.8 mM KOH generated with an eluent generator (Dionex, Thermo Fischer Scientific, MA, USA) (for details see Table S1). 100 mM KOH, for 20 min was used for rinsing the analytical column between each run. Before the analysis of the samples, the system was re-equilibrated with 4.8 mM KOH. During the analysis of the samples, the flow rate was 0.25 mL/min, the temperature of the column was set to 30 °C, and the autosampler temperature set to 5 °C. Calibration curves for monosaccharide standards such as rhamnose, galactose, glucose, xylose, and fructose (Sigma-Aldrich, Saint-Louis, Missouri, USA), were produced independently in triplicates. The appearance of monosaccharides in the biological samples was verified in comparison to reference standards (Fig. 1A).

2.6. Quantification of glucuronic acid (GlcA) and glycerol

GlcA was determined following the same workflow as described above (Fig. S1F) but with a different gradient and eluents for chromatographic separations (Table S2). Glycerol was measured with HPIC using a program involving two eluents, namely NaOH and ultrapure water. The analytical column, Dionex™ CarboPac™ MA1 IC, and its corresponding guard column were from Thermo Fischer Scientific. The flow rate was set at 0.4 mL/min, and the column temperature was kept at 30 °C.

2.7. Bacterial cultivation on various carbon sources

Roseovarius sp. (MS2) were grown aerobically in 50 mL UCM at 20 °C for 18 days and enriched with 1% (*w/v*) of various carbon sources: glycerol [31,32], glucose, rhamnose, galactose, xylose, and fructose. The bacterium was cultivated with each carbon source separately. The bacterial cultures grew in an orbital shaker in 250 mL polystyrene tissue culture flask (Flask T75, Sarstedt, Germany). Bacterial growth was monitored by measuring the optical density at 600 nm (OD_{600}) in a 1-cm polypropylene cell on a UV/Vis spectrophotometer (Genesys, ThermoFisher, Germany). The bacterial growth rate of *Roseovarius* sp. in UCM with 1% glycerol (w/v) as carbon source, was calculated using the following equation; $F(x) = x_{(0)}e^{(\mu * x_t)}$, where $F(x) = OD_{600}$, $x_{(0)}$ is the initial time point of the logarithmic phase, $x_{(t)}$ = the last time point of the logarithmic growth phase and μ = growth rate (change of OD day $^{-1}$).

2.8. Biomass hydrolysis for amino acids quantification

The biomasses of axenic *U. mutabilis* or tripartite community were hydrolyzed according to the manual "Dionex *AAA-Direct*, Amino Acid Analysis System" (Thermo Fischer Scientific, MA, USA) and Kazir's protocol with some modifications [44]. The biomass was dried, grounded, and stored, as described in Section 2.4. The biomass powder (4 ± 0.23 mg) was transferred into 3 mL micro-reaction vials (Sigma Aldrich, MO, USA). The headspaces of the vials were rinsed with N_2 during 10 s. The biomass was added to the vials and incubated in 1 mL of 6 M HCl (Sigma Aldrich, MO, USA) for 16 h at 112 °C (Fig. S1E) with continuous headspace N_2 gas flushing. During the incubation, the vials with the biomasses were in a dry bath with a set of needles for gas flushing (Bio-Base, China). After the incubation, the vials were cooled down to room temperature, and the acid (HCl) was evaporated. The evaporation process was done with N_2 (99%); the gas was purged into open vials through the needles for 3.5 h (flow rate of 4 ± 1 L/min). After complete evaporation of acid, the dry samples were reconstituted with 1 mL of ultrapure water. All samples were diluted with ultrapure water and were filtered with 0.22 μm syringe-filter (Millipore, USA), before the HPIC analysis.

2.9. Amino acids quantification

Analysis of AAs content was performed (Fig. S1F) according to the Kazir's protocol and the manual of Thermo Scientific [44,45]. Total AA content was analyzed with the same equipment and the set up as described in Section 2.5, but with a non-disposable gold AAA™ electrode. The eluent gradient was run, as described in Table S3. The waveform for the electrochemical detector was adopted from the Application Note 163 [46]. The AAs peak areas were compared to commercial AA standard mix (AAS18, Sigma Aldrich, MO, USA). The program was validated with the commercial AA mix (AAS18, Sigma Aldrich, MO, USA). The commercial mix was diluted (1:50, 1:100, 1:250, and 1:1000). Calibration curves were built for 17 AAs: alanine, arginine, aspartate, cysteine, glutamate, glycine, histidine, isoleucine, leucine, lysine, methionine, phenylalanine, proline, serine, threonine, tyrosine, and valine (Fig. 1B). DL-norleucine (Sigma Aldrich, MO, USA) was added to all the samples and standards as an internal standard. The internal standard was used for normalizing the system's sensitivity variations between the samples. The correlation factor for each of them was $R^2 > 99\%$. Cysteine and methionine are probably underestimated [46] because of their sensitivity to the hydrolysis procedure.

2.10. Modeling bioethanol production using flux balance analysis

'BioLego', a software for flux balance analysis [36] was used for the prediction of bioethanol yield. This model relies on the complete metabolic models of the microorganisms with the ability to produce bioethanol. The tested organisms were *Saccharomyces cerevisiae* [47], *Escherichia coli* [48] and *Clostridium acetobutylicum* [49]. Online website was used (http://wassist.cs.technion.ac.il/~edwardv/BioLego/html/BioLego.html) [50] for running the model; the products of *U. mutabilis* axenic and tripartite community biomasses were used as the input. "Other particles" of the model were defined as compounds of the biomass, which do not appear in the default medium. The calculation of the "other particles" was carried out as follows: total chemical components measured in this study was removed from total chemical components in the simulation of default medium (of *U. lactuca*). This difference corresponds to the "other particles" in the default medium.

2.11. Statistical analysis

Tripartite community and axenic culture were carried out in three independent biological replicates. Six individual analytes from each biological replicate were collected for length measurements. The quantification of the monosaccharides, GlcA, glycerol, and AAs for every biological replicate were performed in two technical replicates. Statistical differences between the replicates were measured via a two-tailed Student's *t*-test using Excel software (Microsoft Office 2013). *P* – values < 0.05 were considered as significant difference.

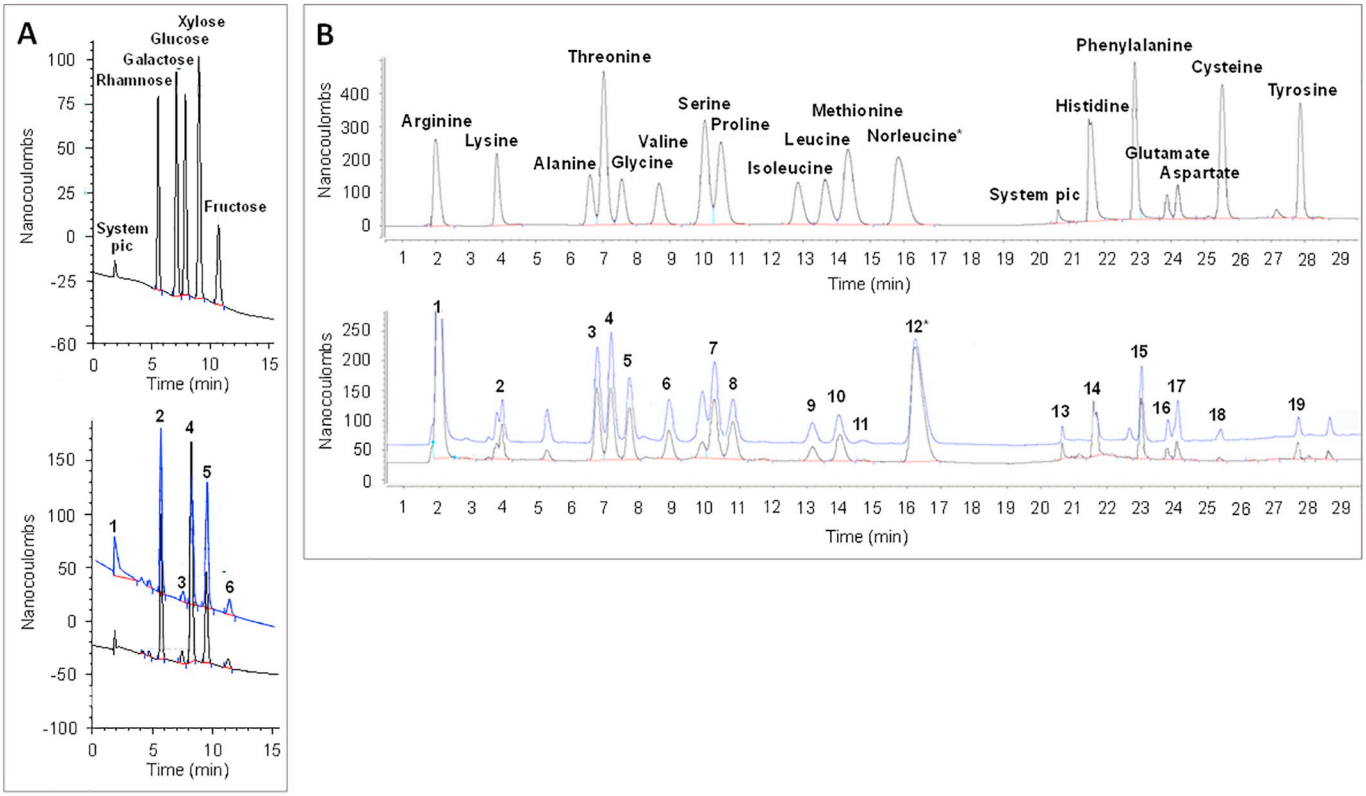

Fig. 1. Ion chromatography for the separation of monosaccharides and amino acids (AAs). Intensity in electric charge (nanocoulombs) over time (in min). A. Monosaccharides separation. The numbers in the chromatogram means: 1 = System peak, 2 = Rhamnose, 3 = Galactose, 4 = Glucose, 5 = Xylose, 6 = Fructose. B. AAs separation. The numbers in the chromatogram means: 1 = Arginine, 2 = Lysine, 3 = Alanine, 4 = Threonine, 5 = Glycine, 6 = Valine, 7 = Serine, 8 = Proline, 9 = Isoleucine, 10 = Leucine, 11 = Methionine, 12* = Norleucine (internal standard), 13 = System peak, 14 = Histidine, 15 = Phenylalanine, 16 = Glutamate, 17 = Aspartate, 18 = Cysteine, 19 = Tyrosine. In A and B the chromatogram on the top, are the separations of monosaccharides or AAs standard mixtures. The chromatograms in the bottom are showing the separation of monosaccharides or AAs in the samples. The blue chromatogram shows the monomers separation in sample of axenic culture. In black are the monomers separation in the sample of tripartite community. (For interpretation of the references to colour in this figure legend, the reader is referred to the web version of this article.)

3. Results and discussion

3.1. *U. mutabilis* growth rate increased under xenic conditions

The growth phase of axenic and xenic *U. mutabilis* culture was determined between 7 and 35 days after the inoculation of axenic gametes with bacteria (Fig. 2). The growth rate of *U. mutabilis* cultivated in the tripartite community was 3.79 mm day $^{-1}$ compared to 0.04 mm day $^{-1}$ in the axenic culture. The maximal length of the thallus reached to 117 ± 19 mm after 35 days within the tripartite community. The average diameter of the callus was only 1.7 ± 0.3 mm in the axenic culture at the end of cultivation (day 63). The effects of bacteria species on *U. mutabilis* growth and morphogenesis corroborated with previous observations, which showed that *Maribacter* sp. and *Roseovarius* sp. (i.e., xenic) modulates the *U. mutabilis* growth and development [26,31,41].

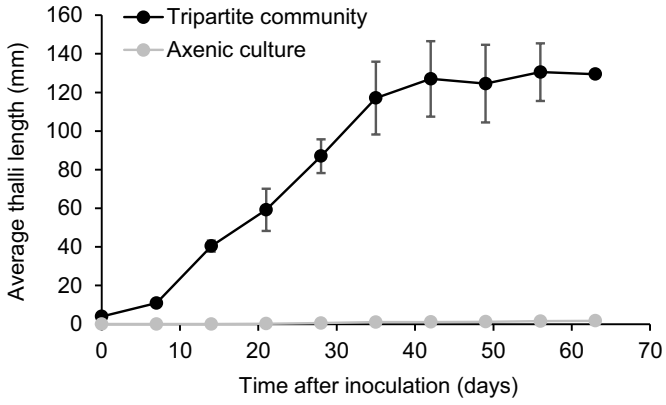

Fig. 2. Growth curve of *Ulva mutabilis*. Average thallus length was measured during growth. *Ulva* biomass was collected from the onset of the algal culture in bioreactors (Day 0) until the mature specimen reached the steady-state growing phase. Error bars represent averages ± standard deviation (n = 18, collected from three biological replications). In axenic cultures, error bars are smaller than the symbol size.

3.2. Xenic conditions affect the monosaccharide and sugar acid profiles of *U. mutabilis* biomass

The monosaccharides, namely, rhamnose, glucose, xylose, fructose, and galactose were identified by comparison to reference standards using HPIC (Fig. 1A, Table S1) and subsequently quantified. After summing up the total amount of monosaccharides, no significant difference was observed in the content, while comparing the axenic and the engineered tripartite community (21.3 ± 0.99 and 23.25 ± 1.00% of DW respectively). Importantly, the percentage of monosaccharides per dry weight (DW) were in the expected range compared to other studies of *Ulva* spp. [7,42,43].

Specific tissue-derived sugars have already been described in *Ulva* spp. several times [11,43,51]. In the current study, the content of rhamnose and fructose did not change either in the xenic or axenic biomasses. Galactose was below the limit of quantitation (LOQ) in all of the samples.

Interestingly, the comparison of the monosaccharides content in the

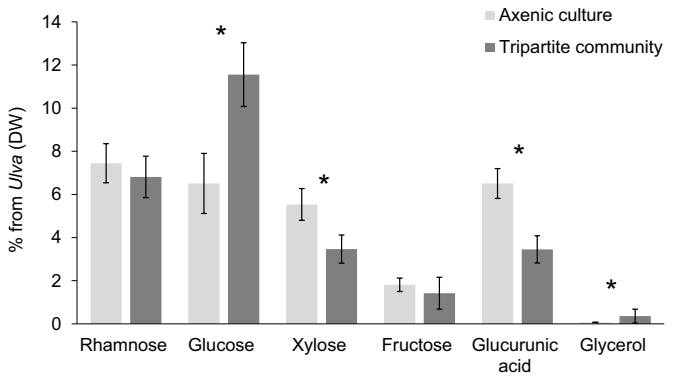

Fig. 3. Monosaccharide, glucuronic acid, and glycerol content in *U. mutabilis* in axenic culture and the tripartite community. *U. mutabilis* axenic culture and the tripartite community biomasses were hydrolyzed after the algae reached the steady-state growth phase, after 8 weeks of cultivation. The monosaccharides were quantified by using HPIC and by comparison to standards. An asterisk indicates the significant difference between the two cultures (two-tailed Student's *t*-test, $P < 0.05$). Error bars represent averages ± standard deviation for $n = 3$ (biological replicates), $n = 2$ (technical replicates).

hydrosylates derived from axenic and tripartite communities of *U. mutabilis* revealed significant monosaccharide type-specific differences (two-tailed Student's *t*-test, $P < 0.05$) in glucose (Fig. 3, Table S4). In detail, when *U. mutabilis* was cultured with the bacteria, its glucose content increased by 77.42 ± 18.6% from 6.51 ± 0.44% to 11.55 ± 0.61% per dry weight (DW). The higher amount of glucose per DW in the tripartite community compared to the axenic samples could be explained by the nitrogen source limited availability (Fig. 2). In a previous study with *U. mutabilis* and the same cultivation conditions, nitrate was entirely utilized by the tripartite community after 20–30 days [31], which might result in a nitrogen limitation. It is known that under nitrogen starvation conditions, *Ulva* accumulates starch [52]. Starch is a polymeric carbohydrate consisting of a large number of glucose units joined by glycosidic bonds, which were hydrolyzed in this study. Interestingly, microbe-algae interactions might trigger starch production, as demonstrated for the green microalgae *Chlorella* spp., which accumulated starch and carbohydrates in the presence of the heterotrophic bacterium *Azospirillum brasilense* [53].

At the same time, the xylose content decreased by 37.37 ± 14.5% from 5.45 ± 0.49 to 3.47 ± 0.18% per DW in the presence of the bacteria. GlcA content per *Ulva* DW in the axenic culture was higher (two-tailed Student's *t*-test, $P < 0.05$) compared to the tripartite community (Fig. 3, S4). The GlcA content in tripartite community biomass decreased by 46.15% from 6.5 ± 0.38 to 3.5 ± 0.46% per DW, respectively. Like glucose, GlcA can be a carbon source for a bioethanol fermentation [54].

Rhamnose xylose and GlcA, are the building blocks of the cell wall polymer ulvan [16,18], which contribute to 8–29% of DW [16,18,55]. In the ratio of xenic culture rhamnose to xylose to GlcA is 1.96:1:1, while in axenic culture 1.34:0.85:1. Previously, the ratio between rhamnose, xylose, and GlcA was detected in *Ulva* wild-type was 3.51:0.92:1 [43]. Therefore, rhamnose to xylose to GlcA ratio in xenic cultures culture is closer to the biomass composition of *Ulva* sp. wild-type that was grown with the natural microbiome. Importantly axenic algae possess malformed cell walls forming protrusions without any further cell differentiation compared to xenic conditions (i.e., with bacteria) [26,41,56]. Therefore, further studies will show how the *Maribacter*-mediated cell wall formation [57] might interfere with the biosynthesis of ulvan and its composition.

These results indicate again that the reduced microbiome of only two bacterial strains is sufficient enough to mimic the natural microbiome and can be used for land-based algal aquacultures under standardized conditions. It is important to note that the bacterial effect on the Ulvan-building block ratio also leads potentially to changes in the Ulvan structure and its functional properties. This evidence could be a key finding for further Ulvan manipulations by using different engineered bacterial consortiums, for controlling the Ulvan properties.

3.3. Xenic growth increases the glycerol content of U. mutabilis biomass

The essential role of glycerol in the cross-kingdom interactions between *U. mutabilis* and its associated bacteria [31,32] motivated the analysis of glycerol. The glycerol content increased by 4.6 times (two-tailed Student's *t*-test, $P < 0.05$) in the tripartite community (0.38 ± 0.11% DW) in comparison to the axenic culture ($0.069 \pm 6.46 \cdot 10^{-3}$% DW) (Figs. 4, S4). The potential amount of glycerol thus increased, which can be secreted into the chemosphere of *U. mutabilis*, providing a carbon source for heterotrophic growth of *Roseovarius* sp. [31].

3.4. Xenic conditions affect the amino acid profile in U. mutabilis biomass

Considering the significant differences in algae development under xenic and axenic conditions [41], we assumed changes in the AA profile

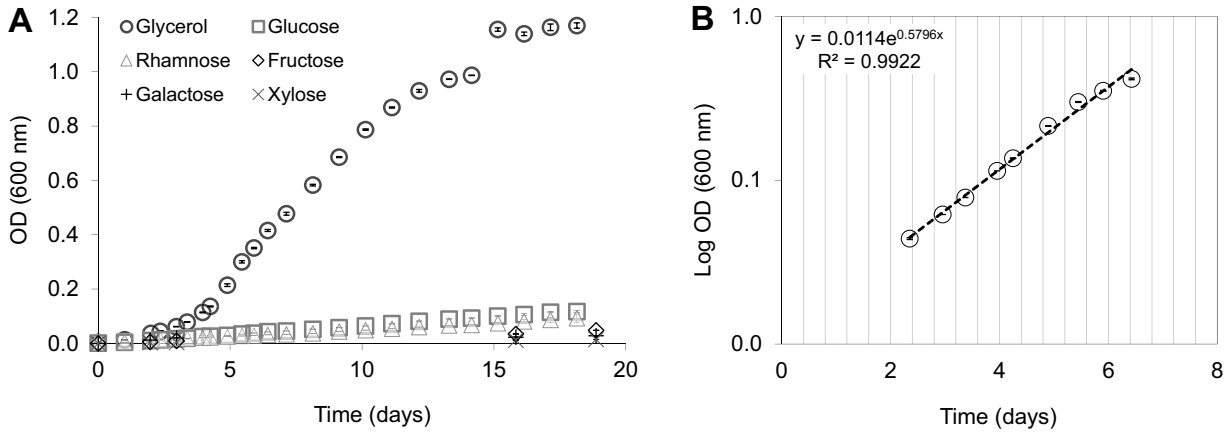

Fig. 4. *Roseovarius* sp. growth with different carbon sources. (A) *Roseovarius* sp. growth in UCM with 1% (*w/v*) various carbon sources; glucose, rhamnose, galactose, fructose, xylose and glycerol during 18 days of cultivation. The bacterial growth was monitored by the OD_{600} and reached the highest optical densities when supplemented with glycerol. With any other tested carbon source, *Roseovarius* sp. grew up to 10% of the final OD_{600} achieved with glycerol as a carbon source. (B) The growth phase of *Roseovarius* sp., which was grown in UCM supplemented with glycerol as a carbon source, from day 2 to 6. Data represent the mean ± standard deviation for $n = 3$ (biological replicates). Error bars are smaller than the symbol size.

Table 1
Amino acid (AA) content comparison between axenic and the tripartite community (mg/g of biomass). Data represent average ± standard deviation for $n = 3$ (biological replicates), $n = 2$ (technical replicates). Hashtag (#) indicates underestimated AA content due to its sensitivity to the hydrolysis treatment. An asterisk (*) indicates the significant difference between the two cultures (two-tailed Student's *t*-test, $P < 0.05$). Dicarboxylic acid (when in nonionic form).

Group of AA		Tripartite community	Axenic culture
Monocarboxylic	Glycine	4.36 ± 0.87	4.86 ± 0.37
	Alanine	7.34 ± 1.65	9.22 ± 0.4
	Valine*	3.81 ± 0.90	5.38 ± 0.44
	Leucine	4.50 ± 0.78	4.40 ± 0.33
	Isoleucine*	2.28 ± 0.49	3.13 ± 0.30
	Total	22.28 ± 4.58	26.99 ± 1.57
Dicarboxylic	Aspartate*	4.37 ± 1.62	7.48 ± 0.78
	Glutamate	4.23 ± 1.73	5.82 ± 0.64
	Total*	8.59 ± 3.34	13.30 ± 1.42
Hydroxy	Threonine*	0.29 ± 0.04	0.48 ± 0.04
	Serine*	3.03 ± 0.38	4.52 ± 0.40
	Total*	3.31 ± 0.42	5.00 ± 0.43
Diamino	Arginine	40.43 ± 5.83	34.70 ± 2.29
	Lysine	2.37 ± 0.54	2.87 ± 0.39
	Total	42.80 ± 6.17	37.57 ± 2.47
Aromatic	Tyrosine*	0.95 ± 0.15	0.33 ± 0.078
	Phenylalanine*	3.34 ± 0.56	4.29 ± 0.40
	Total	4.29 ± 0.70	4.62 ± 0.39
Heterocyclic	Histidine*	0.70 ± 0.09	0.50 ± 0.05
	Proline	2.31 ± 0.34	2.61 ± 0.28
	Total	3.02 ± 0.42	3.11 ± 0.32
Sulfur-containing	Cysteine#	0.30 ± 0.12	0.34 ± 0.05
	Methionine#	0.40 ± 0.11	0.47 ± 0.12
	Total	0.70 ± 0.18	0.81 ± 0.15
	All AA	79.77 ± 6.40	85.24 ± 3.94

as well. The AA profile might change according to the conditions synthesis and activity of some enzymes, gene expression, and redox-homeostasis [58]. In this study, 17 AAs were quantified (Table 1, Fig. 1B). The total AA (sum of 17 AAs) content of the tripartite community and axenic culture did not differ significantly (two-tailed, Student's t-test, $P > 0.05$). Tyrosine (aromatic) and histidine (heterocyclic) significantly increased (two-tailed Student's *t*-test, $P < 0.05$) by 191 ± 61% (from 0.33 ± 0.078 to 0.95 ± 0.15 mg/g of *Ulva* DW) and by 40 ± 26% (from 0. 5 ± 0.05 to 0.7 ± 0.09 mg/g of *Ulva* DW respectively in xenic culture). The content of six AAs significantly decreased (by about one-third) in the stationary phase (two-tailed Student's *t*-test, $P < 0.05$). The valine content decreased by 29 ± 24%, isoleucine, decreased by 27 ± 27%, aspartate, decreased by 42 ± 23%, threonine, decreased by 40 ± 11%, serine, decreased by 33 ± 16%, and phenylalanine, decreased by 22 ± 19% in the tripartite community. The content of arginine, lysine, alanine, glycine, proline, leucine, and glutamate did not depend on bacterial treatment. Clustering the AAs into groups (Table 1) showed that the total dicarboxylic- and the total hydroxy-AAs were significantly higher (two-tailed, Student's t-test, $P < 0.05$) in the axenic culture. The total content of the groups, including of monocarboxylic-, diamino-, aromatic-, heterocyclic-, and sulfur-AAs, were not significantly different between xenic and axenic cultures. In a previous study, a dramatic difference was observed in the intercellular content of AA in diatoms upon bacterial addition [59]. The profile of intercellular dissolved AAs in diatoms considerably changed after co-cultivating the diatoms with bacteria [59]. The intercellular content of histidine was significantly higher in axenic culture, and the content of isoleucine was much higher in the consortium of diatoms and bacteria [59]. In our study, an opposite pattern was observed for both AAs.

3.5. Change of profile in Ulva photosynthates indicates the need for bacterial growth

Algae provide photosynthate for heterotrophic bacteria in symbiosis. Besides, algal compounds are utilized by the bacteria during the algal decomposition [60]. Therefore, we studied whether the bacterium-induced change in *Ulva*'s chemical profile of the photosynthate could be correlated to the bacterial eco-physiological function in the cross-kingdom interaction [31,32]. In other words, if the bacterium induces the changes in the algae biomass for its benefits, it could be the explanation for bacterial influence on the algal monosaccharides composition during the algal growth (Fig. 3). After testing the growth of *Roseovarius* sp. in *Ulva* culture medium (UCM) with different major *Ulva*'s monosaccharides as a carbon source (Fig. 4A), only weak bacterial growth was measured. Only glucose contributed slightly to the growth of *Roseovarius* sp. as reported by Spoerner et al. (2012) [41], but the optical density (OD_{600}) did not reach values higher than 0.15. The inability to grow sufficiently on glucose was also found for *Roseovarius mucosus* [61]. We thus argue that *Roseovarius* sp. (MS2) did not gain benefit from the algal monosaccharides. However, after 18 days of cultivation with 1% (*w/v*) glycerol in UCM, the OD_{600} reached 1.17 (±8.16 E−03), showing the typical growth curve (Fig. 4A). The growth

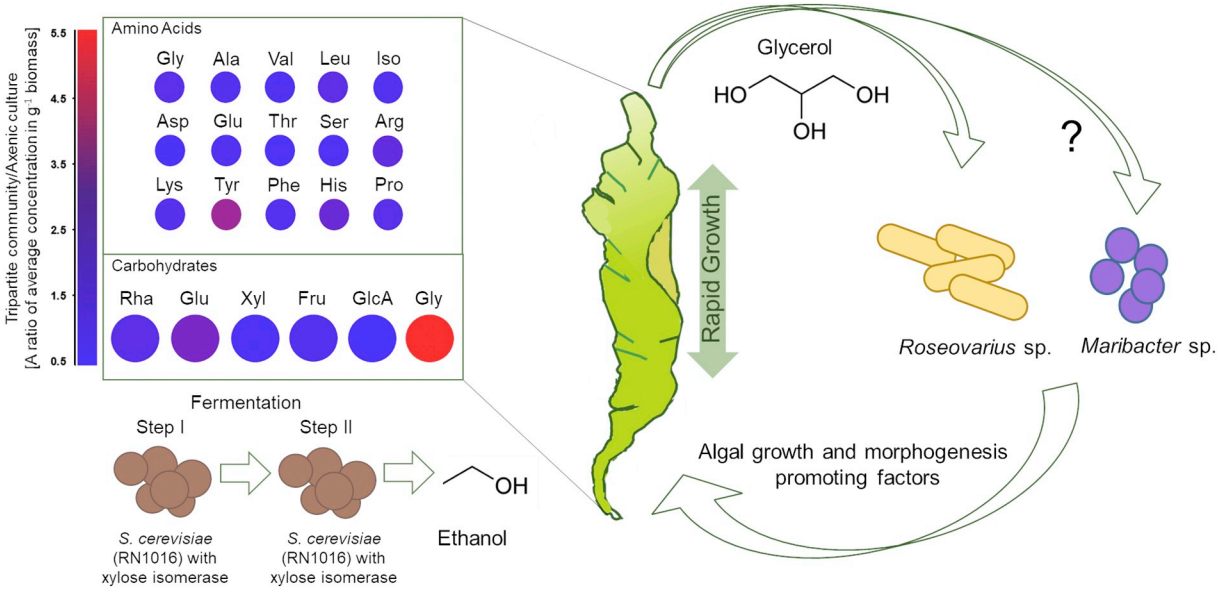

Fig. 5. Schematic diagram summarizing the *U. mutabilis* and it's associated bacteria interactions and the metabolic model analysis.

rate was 0.58 (change of OD_{600} per day) (Fig. 4B). It means that *Roseovarius* sp. (MS2) efficiently utilized and grew on glycerol as the only carbon source (Figs. 4, and 5) [31,32]. The current data support the previous report, where bacteria promote algal growth and morphogenesis [31,41,62,63]. In return, *Ulva* can provide the bacterial carbon source, as indicated by the elevated amounts of glycerol in the tissue. It supports the observation that algae growth-promoting bacteria are enriched in intensive land-based algal aquacultures compared to the seawater supplied to the aquaculture system [64].

At the same time, *Maribacter* sp. (MS6) did not grow on UCM supplemented with different monosaccharides or glycerol and needs complex media such as marine broth [32,Wichard and Weiss pers. observation]. The *Maribacter polisphoniae* might be an interesting exception because it grows on glycerol [65].

Overall, the insights in the algal-bacterial interaction pave the way to improved culture conditions, which might yield higher amounts of glycerol. Importantly, glycerol is an efficient carbon source for fermentation and biofuels production, such as bioethanol, under standardized conditions [66].

Our study paves the way for microbiome engineering to develop *Ulva* as a cash crop. *Ulva* affects its microbiome in intensive algal aquaculture, which promotes beneficial bacteria for the alga [67]. Inoculates of those bacteria need to be applied in order to test their effect on growth and the production of specific constituents. Indeed, our results support that the presence of bacteria is associated with changes in the content of photosynthates. Improved plant breeding has already been performed with plant probiotic bacteria successfully [68]. Also, bacterial-based biofertilizers have been considered as a promising application for increasing the yield of terrestrial crops in an environmentally-friendly manner, improving the plant's nutrient availability, and making the plant biomass to be more efficient for human needs [69]. We believe that the current data are a first step towards the development of algae promoting probiotics.

3.6. Simulation of bioethanol fermentation from Ulva biomass using metabolic flux balance analysis

The bioethanol yields from xenic and axenic cultured were estimated *in-silico* using 'BioLego' [36,50] (Table S5). In all simulations, we used the fermentation broth composition based on the measured values of monosaccharides, GlcA, and glycerol, and AAs in both biomasses. The fermentation was simulated for *S. cerevisiae* wild type (WT) [47] and recombinant strain with xyole-isomerase from *Piromyces* sp. [70], *E. coli* [48] and *C. acetobutylicum* [49].

Tripartite community derived *U. mutabilis* was a preferred feedstock for bioethanol production in most simulations. In those simulations, the majority of the bioethanol yield relayed on glucose and glycerol metabolism. Those two components were higher in *U. mutabilis* from the tripartite community (Table S4). Among all combinations, the two-step fermentation with the same organisms (Table S5, simulation no. 9, and Fig. 5) *S. cerevisiae* RN1016 (+xylose isomerase) resulted in the highest bioethanol yield, of 85.62 g/kg (using tripartite community). It is probably due to the additional pathways leading to bioethanol production in the presence of xylose isomerase [36,70]. The highest difference in bioethanol yields between approaches using the *Ulva* biomass from the tripartite community or axenic culture was detected in single-step or two-step fermentation with *C. acetobutylicum* (Table S5, simulations No. 16 and 20).

Only in simulations where C. acetobutylicum was used in the first step and *S. cerevisiae* RN1016 (+xylose isomerase) or *E. coli* used in the second step, the axenic biomass led to larger bioethanol yield (although the total yields are low: 16.95–30.45 g/kg). Those exceptional simulations results might be explained by available carbon source during the fermentation. The first-step, contributed to higher bioethanol yield, using the tripartite community (3.85 g/kg) than from axenic culture (2.25 g/kg). At the second-step, more bioethanol was produced using axenic culture (with *S. cerevisiae* RN1016 (+xylose isomerase) 28.2 g/kg or 14.7 g/kg with *E. coli*) than from tripartite community (with *S. cerevisiae* 19.5 g/kg or 11.54 g/kg with *E. coli*). On the first-step, C. acetobutylicum consumed all carbon sources except the xylose, which produced a relatively low bioethanol yield. C. acetobutylicum was thus the weakest bioethanol producer among all tested organisms so far [49,71–73]. In the second fermentation step, the bioethanol production was based on xylose metabolism. The larger the xylose content, the higher the yield of bioethanol in this fermentation step. Therefore, the usage of axenic biomass was probably more efficient for bioethanol production. In those two exceptional simulations, numbers 18 and 19 (Table S5), the bioethanol yield consuming axenic culture was higher in 30.4 and 10.1%, respectively, than consuming tripartite community biomass.

4. Conclusion

The current study demonstrates that macroalgae *U. mutabilis* associated bacteria modulate *Ulva* growth rate and the major photosynthate components. The studied constituents were monosaccharides, glycerol, glucuronic acid, and amino acids content after cultivation during the algal stationary phase before the occurrence of the next sporulation event. The quantity of the compounds was normalized to the dry weight of the harvested biomass. The tissue of *U. mutabilis* cultivated with the bacteria *Maribacter* sp. and *Roseovarius* sp. was enriched with glucose, glycerol, histidine, and tyrosine but decreased in the content of xylose, GlcA, valine, isoleucine, aspartate, threonine, serine, and phenylalanine compared to the axenic culture. The addition of two bacteria to *U. mutabilis* cultivation changed the ratio of rhamnose/xylose/GlcA, which became closer to the ratio found in *Ulva* with its natural microbiome. Although the factors are unknown, which are required to understand the complicated cause-effect relationship of bacteria-algae interactions, our observations linked the presence of the bacteria in the environment of *Ulva* with the formation of an essential constituent of the algal cell wall, development, and growth. Glycerol was the most affected component in the algal photosynthate by the bacteria. As glycerol is the preferred component for the growth of *Roseovarius* sp. (MS2), it is an additional insight into the glycerol function in the cross-kingdom interactions. The metabolic model simulations of *U. mutabilis* fermentation with *S. cerevisiae*, *E. coli*, and *C. acetobutylicum*, suggested the higher bioethanol yield after fermenting in xenic than axenic culture biomass. The highest yields were estimated from a two-step fermentation with *S. cerevisiae* (RN1016) that included the xylose isomerase.

In summary, our results are a valuable example of how the understanding of chemical ecology can help us to use associated macroalgal bacterial interactions to adjust the biomass feedstock for bioethanol production. Overall, this type of modulation opens new pathways for developing an efficient biorefinery based on macroalgae.

Authors' contributions

M.P. conceived the project, performed the chemical analysis and model calculations. G.C. carried out the cultivation and harvested the algae for further sample preparation. N.D. carried out the bacterial cultivation and their growth measurements. T.W. supervised the project in Jena during the Short Term COST Scientific Mission. A.G. conceived and supervised the project. All authors have analyzed the data and drafted the paper.

Declaration of competing interest

The authors declare no conflict of interest.

Acknowledgements

This research financed by Israel Ministry of Science, Technology and Space (A.G., M.P.). This article is based upon work from COST Action FA1406 Phycomorph, supported by COST (European Cooperation in Science and Technology, www.cost.eu). This work was also partly supported by the European Union's Horizon 2020 - Research and Innovation Framework Programme under the Marie Sklodowska-Curie grant agreement No.642575 (G.C., T.W.) and by the Deutsche Forschungsgemeinschaft through CRC 1127 ChemBioSys (N.D., T.W.). Thanks to Arthur Robin for assisting with the sugars and AAs separation, to Dr. Edward Vitkin for supporting with 'BioLego' model (A.G., M.P.)

Appendix A. Supplementary data

Supplementary data to this article can be found online at https://doi.org/10.1016/j.algal.2020.101945.

References

[1] World Energy Council, World energy resources, http://www.worldenergy.org/wp-content/uploads/2013/09/Complete_WER_2013_Survey.pdf, (2016).
[2] T.J. Wilbanks, S.J. Fernandez, Climate Change and Energy Supply and Use: Technical Report for the U.S Department of Energy in Support of the National Climate Assessment, (2014), https://doi.org/10.5822/978-1-61091-556-4.
[3] D. Pimentel, Ethanol fuels: energy balance, economics, and environmental impacts are negative, Nat. Resour. Res. 12 (2003) 127–134.
[4] FAO, The State of Food and Agriculture, (2016) (ISBN:978-92-5-107671-2 I).
[5] B. Moss, Water pollution by agriculture, Philos. Trans. R. Soc. B Biol. Sci. 363 (2008) 659–666.
[6] A. Bruhn, J. Dahl, H.B. Nielsen, L. Nikolaisen, M.B. Rasmussen, S. Markager, B. Olesen, C. Arias, P.D. Jensen, Bioenergy potential of *Ulva lactuca*: biomass yield, methane production and combustion, Bioresour. Technol. 102 (2011) 2595–2604.
[7] H. van der Wal, B.L.H.M. Sperber, B. Houweling-Tan, R.R.C. Bakker, W. Brandenburg, A.M. López-Contreras, Production of acetone, butanol, and ethanol from biomass of the green seaweed *Ulva lactuca*, Bioresour. Technol. 128 (2013) 431–437.
[8] A. Golberg, E. Vitkin, G. Linshiz, S.A. Khan, N.J. Hillson, Z. Yakhini, M.L. Yarmush, Proposed design of distributed macroalgal biorefineries: thermodynamics, bio-conversion technology, and sustainability implications for developing economies, Biofuels Bioprod. Biorefin. 8 (2014) 67–82.
[9] S. Kraan, Mass-cultivation of carbohydrate rich macroalgae, a possible solution for sustainable biofuel production, Mitig. Adapt. Strateg. Glob. Chang. 18 (2013) 27–46.
[10] Y. Lehahn, K.N. Ingle, A. Golberg, Global potential of offshore and shallow waters macroalgal biorefineries to provide for food, chemicals and energy: feasibility and sustainability, Algal Res. 17 (2016) 150–160.
[11] P. Bikker, M.M. van Krimpen, P. van Wikselaar, B. Houweling-Tan, N. Scaccia, J.W. van Hal, W.J.J. Huijgen, J.W. Cone, A.M. Lopez-Contreras, Biorefinery of the green seaweed *Ulva lactuca* to produce animal feed, chemicals and biofuels, J. Appl. Phycol. 28 (2016) 3511–3525.
[12] J.E. Vermaat, K. Sand-Jensen, Survival, metabolism and growth of *Ulva lactuca* under winter conditions: a laboratory study of bottlenecks in the life cycle, Mar. Biol. 95 (1987) 55–61.
[13] M.D. Guiry, G.M. Guiry, AlgaeBase, World-Wide Electron. Publ. Natl. Univ. Ireland, Galw, (2018).
[14] A.F. Abdel-Fattah, M. Edrees, A study on the polysaccharide content of *Ulva lactuca* L, Qual. Plant. Mater. Veg. 22 (1972) 15–22.
[15] L. Nikolaisen, P. Daugbjerg Jensen, K. Svane Bech, J. Dahl, J. Busk, T. Brødsgaard, M.B. Rasmussen, A. Bruhn, A.-B. Bjerre, H. Bangsø Nielsen, Energy Production from Marine Biomass (*Ulva lactuca*), Danish Technological Institute, 2011.
[16] A. Robic, D. Bertrand, J.F. Sassi, Y. Lerat, M. Lahaye, Determination of the chemical composition of ulvan, a cell wall polysaccharide from *Ulva* spp. (Ulvales, Chlorophyta) by FT-IR and chemometrics, J. Appl. Phycol. 21 (2009) 451–456.
[17] M. Lahaye, B. Ray, S. Baumberger, B. Quemener, M.A.V. Axelos, Chemical characterisation and gelling properties of cell wall polysaccharides from species of *Ulva* (Ulvales, Chlorophyta), Fifteenth Int. Seaweed Symp, Springer, 1996, pp. 473–480.
[18] A. Robic, J. Sassi, P. Dion, Y. Lerat, M. Lahaye, Seasonal variability of physico-chemical and rheological properties of Ulvan in two *Ulva* species (Chlorophyta) from the Brittany Coast 1, J. Phycol. 45 (2009) 962–973.
[19] A.F. Mohsen, A.H. Nasr, A.M. Metwalli, Effect of temperature variations on growth, reproduction, amino acid synthesis, fat and sugar content in *Ulva fasciata* delile plants, Hydrobiologia 42 (1973) 451–460.
[20] M. Ganesan, O.P. Mairh, K. Eswaran, P.V. Rao, Effect of Salinity, Light Intensity and Nitrogen Source on Growth and Composition of *Ulva fasciata* Delile (Chlorophyta, Ulvales), (1999).
[21] A. Chemodanov, G. Jinjikhashvily, O. Habiby, A. Liberzon, A. Israel, Z. Yakhini, A. Golberg, Net primary productivity, biofuel production and CO_2 emissions reduction potential of *Ulva* sp. (Chlorophyta) biomass in a coastal area of the Eastern Mediterranean, Energy Convers. Manag. 148 (2017) 1497–1507.
[22] M. Naldi, P.A. Wheeler, Changes in nitrogen pools in *Ulva fenestrata* (Chlorophyta) and *Gracilaria pacifica* (Rhodophyta) under nitrate and ammonium enrichment, J. Phycol. 35 (1999) 70–77.
[23] F.E. Msuya, A. Neori, Effect of water aeration and nutrient load level on biomass yield, N uptake and protein content of the seaweed *Ulva lactuca* cultured in sea-water tanks, J. Appl. Phycol. 20 (2008) 1021–1031.
[24] L. Korzen, A. Abelson, A. Israel, Growth, protein and carbohydrate contents in *Ulva rigida* and *Gracilaria bursa-pastoris* integrated with an offshore fish farm, J. Appl. Phycol. 28 (2016) 1835–1845.
[25] K.N. Ingle, M. Polikovsky, A. Chemodanov, A. Golberg, Marine integrated pest management (MIPM) approach for sustainable seagriculture, Algal Res. 29 (2018) 223–232.
[26] T. Wichard, Exploring bacteria-induced growth and morphogenesis in the green macroalga order Ulvales (Chlorophyta), Front. Plant Sci. 6 (2015) 86.
[27] R.P. Singh, C.R.K. Reddy, Seaweed–microbial interactions: key functions of seaweed-associated bacteria, FEMS Microbiol. Ecol. 88 (2014) 213–230.
[28] F. Goecke, A. Labes, J. Wiese, J.F. Imhoff, Chemical interactions between marine macroalgae and bacteria, Mar. Ecol. Prog. Ser. 409 (2010) 267–299.
[29] S. Egan, T. Harder, C. Burke, P. Steinberg, S. Kjelleberg, T. Thomas, The seaweed holobiont: understanding seaweed–bacteria interactions, FEMS Microbiol. Rev. 37 (2013) 462–476.
[30] K. Spilling, J. Titelman, T.M. Greve, M. Kühl, Microsensor measurements of the external and internal microenvironment of *Fucus Vesiculosus* (Phaeophyceae) 1, J. Phycol. 46 (2010) 1350–1355.
[31] T. Alsufyani, A. Weiss, T. Wichard, Time course exo-metabolomic profiling in the green marine macroalga *Ulva* (Chlorophyta) for identification of growth phase-dependent biomarkers, Mar. Drugs. 15 (2017) 14.
[32] R.W. Kessler, A. Weiss, S. Kuegler, C. Hermes, T. Wichard, Macroalgal–bacterial interactions: role of dimethylsulfoniopropionate in microbial gardening by *Ulva* (Chlorophyta), Mol. Ecol. 27 (2018) 1808–1819.
[33] E.C. Sonnenschein, C.B.W. Phippen, M. Bentzon-Tilia, S.A. Rasmussen, K.F. Nielsen, L. Gram, Phylogenetic distribution of roseobacticides in the *Roseobacter* group and their effect on microalgae, Environ. Microbiol. Rep. 10 (2018) 383–393.
[34] D.J. Murphy, Structure, function and biogenesis of storage lipid bodies and oleosins in plants, Prog. Lipid Res. 32 (1993) 247–280.
[35] I.A. Graham, Seed storage oil mobilization, Annu. Rev. Plant Biol. 59 (2008) 115–142.
[36] E. Vitkin, A. Golberg, Z. Yakhini, BioLEGO—a web-based application for biorefinery design and evaluation of serial biomass fermentation, Technology 3 (2015) 89–98.
[37] G. Nilsen, Ø. Nordby, A sporulation-inhibiting substance from vegetative thalli of the green alga *Ulva mutabilis*, Føyn, Planta 125 (1975) 127–139.
[38] B. Føyn, Über die Sexualität und den Generationswechsel von *Ulva mutabilis* (N.S.), Arch, Für Protistenkd 102 (1958) 473–480.
[39] T. Wichard, W. Oertel, Gametogenesis and gamete release of *Ulva mutabilis* and *Ulva lactuca* (Chlorophyta): regulatory effects and chemical characterization of the "swarming inhibitor" 1, J. Phycol. 46 (2010) 248–259.
[40] G. Califano, T. Wichard, Preparation of axenic cultures in *Ulva* (Chlorophyta), Protoc. Macroalgae Res. (2018) 159–171.
[41] M. Spoerner, T. Wichard, T. Bachhuber, J. Stratmann, W. Oertel, Growth and thallus morphogenesis of *Ulva mutabilis* (Chlorophyta) depends on a combination of two bacterial species excreting regulatory factors, J. Phycol. 48 (2012) 1433–1447.
[42] R. Jiang, Y. Linzon, E. Vitkin, Z. Yakhini, A. Chudnovsky, A. Golberg, Thermochemical hydrolysis of macroalgae *Ulva* for biorefinery: Taguchi robust design method, Sci. Rep. 6 (2016).
[43] A. Robin, P. Chavel, A. Chemodanov, A. Israel, A. Golberg, Diversity of monosaccharides in marine macroalgae from the Eastern Mediterranean Sea, Algal Res. 28 (2017) 118–127.
[44] T.F.S. Inc, Dionex AAA-direct, amino acid analysis system (product manual), https://assets.thermofisher.com/TFS-Assets/CMD/manuals/Man-031481-AAA-Direct-Man031481-EN.pdf, (2018).
[45] M. Kazir, Y. Abuhassira, A. Robin, O. Nahor, J. Luo, A. Israel, A. Golberg, Y.D. Livney, Extraction of proteins from two marine macroalgae, *Ulva* sp. and *Gracilaria* sp., for food application, and evaluating digestibility, amino acid composition and antioxidant properties of the protein concentrates, Food Hydrocoll. 87 (2019) 194–203.
[46] Dionex Corporation, Determination of Protein Concentration Using AAA-Direct (Application Note 163), (2004).
[47] B.D. Heavner, K. Smallbone, B. Barker, P. Mendes, L.P. Walker, Yeast 5–an expanded reconstruction of the *Saccharomyces cerevisiae* metabolic network, BMC Syst. Biol. 6 (2012) 55.
[48] J.D. Orth, T.M. Conrad, J. Na, J.A. Lerman, H. Nam, A.M. Feist, B.Ø. Palsson, A comprehensive genome-scale reconstruction of *Escherichia coli* metabolism—2011, Mol. Syst. Biol. 7 (2011) 535.
[49] M.J. McAnulty, J.Y. Yen, B.G. Freedman, R.S. Senger, Genome-scale modeling using flux ratio constraints to enable metabolic engineering of clostridial metabolism *in silico*, BMC Syst. Biol. 6 (2012) 42.
[50] E. Vitkin, BioLEGO, http://wassist.cs.technion.ac.il/~edwardv/BioLego/html/BioLego.html, (2015) , Accessed date: 11 March 2015.
[51] E. Percival, B. Smestad, Photosynthetic studies on *Ulva lactuca*, Phytochemistry 11 (1972) 1967–1972.
[52] M. Prabhu, A. Chemodanov, R. Gottlieb, M. Kazir, O. Nahor, M. Gozin, A. Israel, Y.D. Livney, A. Golberg, Starch from the sea: the green macroalga *Ulva* sp. as a potential source for sustainable starch production from the sea in marine biorefineries, Algal Res. 37 (2019) 215–227.

[53] F.J. Choix, L.E. de-Bashan, Y. Bashan, Enhanced accumulation of starch and total carbohydrates in alginate-immobilized *Chlorella* spp. induced by *Azospirillum brasilense*: II. Heterotrophic conditions, Enzym. Microb. Technol. 51 (2012) 300–309.
[54] H.G. Lawford, J.D. Rousseau, Fermentation of biomass-derived glucuronic acid bypet expressing recombinants of *E. coli* B, Appl. Biochem. Biotechnol. 63 (1997) 221–241.
[55] M. Tako, M. Tamanaha, Y. Tamashiro, S. Uechi, Structure of ulvan isolated from the edible green seaweed, *Ulva pertusa*, Adv. Biosci. Biotechnol. 6 (2015) 645.
[56] A. Weiss, R. Costa, T. Wichard, Morphogenesis of *Ulva mutabilis* (Chlorophyta) induced by *Maribacter* species (Bacteroidetes, Flavobacteriaceae), Bot. Mar. 60 (2017) 197–206.
[57] T. Alsufyani, G. Califano, M. Deicke, J. Grueneberg, A. Weiss, A.H. Engelen, M. Kwantes, J.F. Mohr, J.F. Ulrich, T. Wichard, Macroalgal–bacterial interactions: identification and role of thallusin in morphogenesis of the seaweed *Ulva* (Chlorophyta), J. Exp. Bot. (eraa066) (2020).
[58] V.K. Rai, Role of amino acids in plant responses to stresses, Biol. Plant. 45 (2002) 481–487.
[59] C.G. Bruckner, C. Rehm, H. Grossart, P.G. Kroth, Growth and release of extracellular organic compounds by benthic diatoms depend on interactions with bacteria, Environ. Microbiol. 13 (2011) 1052–1063.
[60] B.A. Lomstein, L.B. Guldberg, A.-T.A. Neubauer, J. Hansen, A. Donnelly, R.A. Herbert, P. Viaroli, G. Giordani, R. Azzoni, R. de Wit, K. Finster, Benthic decomposition of *Ulva lactuca*: a controlled laboratory experiment, Aquat. Bot. 85 (2006) 271–281.
[61] H. Biebl, M. Allgaier, H. Lünsdorf, R. Pukall, B.J. Tindall, I. Wagner-Döbler, *Roseovarius mucosus* sp. nov., a member of the *Roseobacter* clade with trace amounts of bacteriochlorophyll a, Int. J. Syst. Evol. Microbiol. 55 (2005) 2377–2383.
[62] F. Ghaderiardakani, J.C. Coates, T. Wichard, Bacteria-induced morphogenesis of *Ulva intestinalis* and *Ulva mutabilis* (Chlorophyta): a contribution to the lottery theory, FEMS Microbiol. Ecol. 93 (2017).
[63] T. Wichard, B. Charrier, F. Mineur, J.H. Bothwell, O. De Clerck, J.C. Coates, The green seaweed *Ulva*: a model system to study morphogenesis, Front. Plant Sci. 6 (2015) 72.
[64] F. Ghaderiardakani, G. Califano, J.F. Mohr, M.H. Abreu, J.C. Coates, T. Wichard, Analysis of algal growth- and morphogenesis-promoting bacterial factors (AGPFs) in an integrated multi-trophic aquaculture system for farming the green seaweed *Ulva*, Aquac. Environ. Interact. 11 (2019) 375–391.
[65] O.I. Nedashkovskaya, M. Vancanneyt, P. De Vos, S.B. Kim, M.S. Lee, V.V. Mikhailov, *Maribacter polysiphoniae* sp. nov., isolated from a red alga, Int. J. Syst. Evol. Microbiol. 57 (2007) 2840–2843.
[66] A. Murarka, Y. Dharmadi, S.S. Yazdani, R. Gonzalez, Fermentative utilization of glycerol by *Escherichia coli* and its implications for the production of fuels and chemicals, Appl. Environ. Microbiol. 74 (2008) 1124–1135.
[67] G. Califano, M. Kwantes, M.H. Abreu, R. Da Silva Costa, T. Wichard, Cultivating the macroalgal holobiont: effects of integrated multi-trophic aquaculture on the microbiome of *Ulva rigida* (chlorophyta), Front. Mar. Sci. 7 (2020) 52.
[68] J.A. Mukta, M. Rahman, A.A. Sabir, D.R. Gupta, M.Z. Surovy, M. Rahman, M.T. Islam, Chitosan and plant probiotics application enhance growth and yield of strawberry, Biocatal. Agric. Biotechnol. 11 (2017) 9–18.
[69] P. García-Fraile, E. Menéndez, L. Celador-Lera, A. Díez-Méndez, A. Jiménez-Gómez, M. Marcos-García, X.A. Cruz-González, P. Martínez-Hidalgo, P.F. Mateos, R. Rivas, Bacterial probiotics: a truly green revolution, Probiotics Plant Heal, Springer, 2017, pp. 131–162.
[70] H.R. Harhangi, A.S. Akhmanova, R. Emmens, C. Van Der Drift, W.T.A.M. De Laat, J.P. Van Dijken, M.S.M. Jetten, J.T. Pronk, H.J.M. Op Den Camp, Xylose metabolism in the anaerobic fungus *Piromyces* sp. strain E2 follows the bacterial pathway, Arch. Microbiol. 180 (2003) 134–141.
[71] J. Lee, H. Yun, A.M. Feist, B.Ø. Palsson, S.Y. Lee, Genome-scale reconstruction and in silico analysis of the *Clostridium acetobutylicum* ATCC 824 metabolic network, Appl. Microbiol. Biotechnol. 80 (2008) 849–862.
[72] Y. Kim, L.O. Ingram, K.T. Shanmugam, Construction of an *Escherichia coli* K-12 mutant for homoethanologenic fermentation of glucose or xylose without foreign genes, Appl. Environ. Microbiol. 73 (2007) 1766–1771.
[73] F. Talebnia, C. Niklasson, M.J. Taherzadeh, Ethanol production from glucose and dilute-acid hydrolyzates by encapsulated *S. cerevisiae*, Biotechnol. Bioeng. 90 (2005) 345–353.